vorticity plots also suggest that the downstream formation length of vortices decreases with increasing reduced frequency.

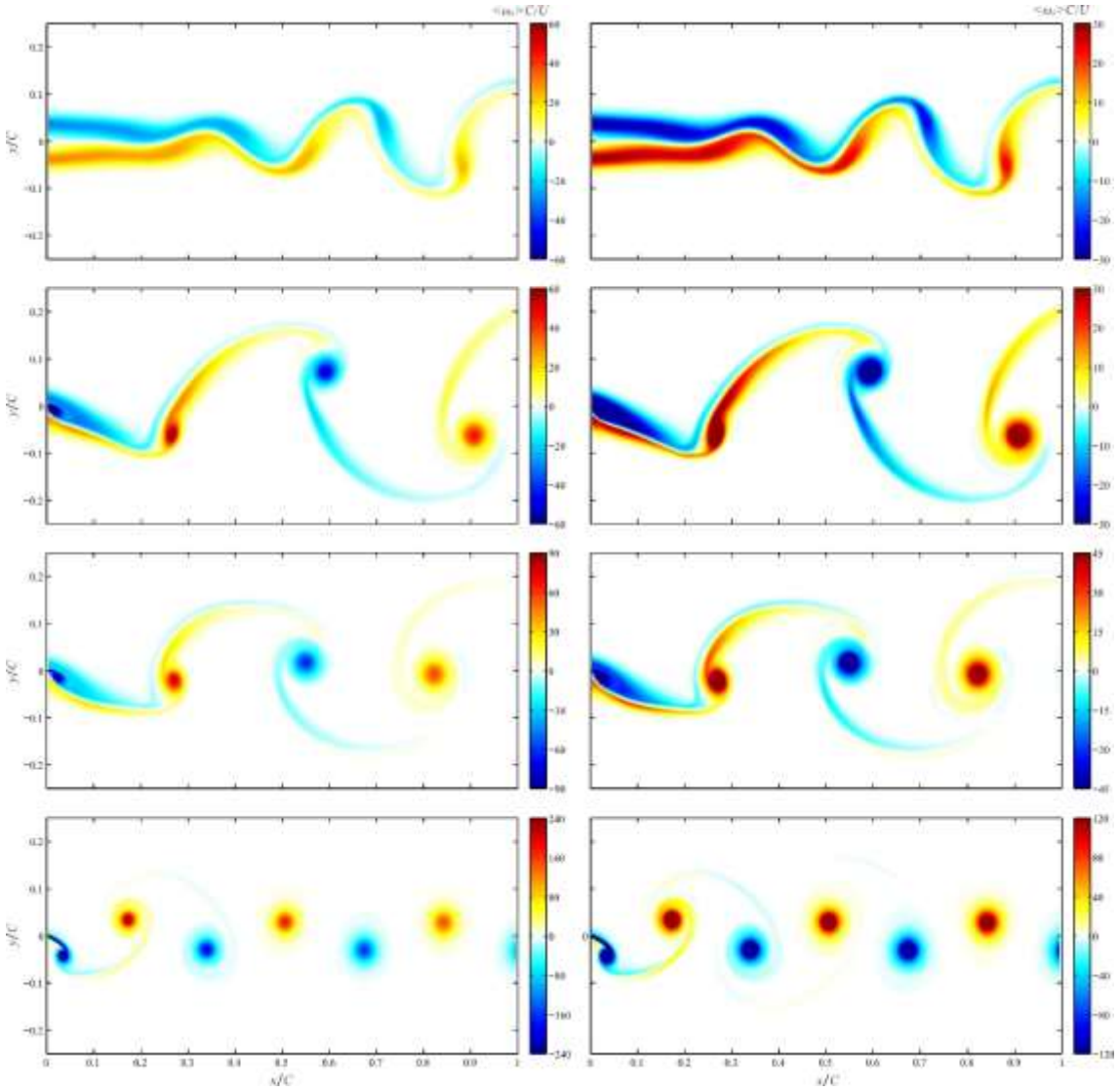

Fig. 3 Phase-averaged vorticity contours in the near wake of static and pitching airfoil.

The non-dimensional mean and fluctuating vorticity, $\omega_{avg}C/U_0$ and $\omega_{r.m.s.}C/U_0$ for oscillating airfoil with three reduced frequencies of k = 5.2, 5.7 and 11.5 are shown in Fig. 4. The mean and r.m.s. vorticity fields of the stationary airfoil at zero AOA are also demonstrated as a supplement. In the case of stationary airfoil, the boundary layer vorticity initiating from the sides of airfoil left the trailing edge quite steadily into the near wake while reducing in peak level with downstream evolution. The mean vorticity fields of low reduced frequency case (k = 5.2) was characterized by the transverse spreading and downstream decaying of braid regions initiated from the trailing edge. The mean vorticity within these regions is of opposite sign to the corresponding boundary later vorticity on the same side. Two well-defined mean vorticity peaks of opposite sign can be identified in second half chord downstream distance where the isolated vortices

have formed in this region. The spacing between the peaks initially increases, followed by a decrease to an asymptotic value by x/C = 1.

The aforementioned behaviors about the characteristics of the mean vorticity field in the near wake region also holds for the case of k = 5.7. The unique feature of this case is the fact that the mean vorticity is nearly zero for x/C > 0.75 indicating the perfect alignment of alternating vortices. In the high reduced frequency case (k = 11.5), two well-defined peaks of opposite sign right at the trailing edge is developed in the mean vorticity filed, indicating the rapid shedding of the isolated vortices at trailing edge. A wavy pattern can be identified for the spacing between the mean vorticity peaks in the near wake before it reaches to a fixed spacing in the far wake. The r.m.s. vorticity field also shows the same initial wavy pattern existed in the mean vorticity.

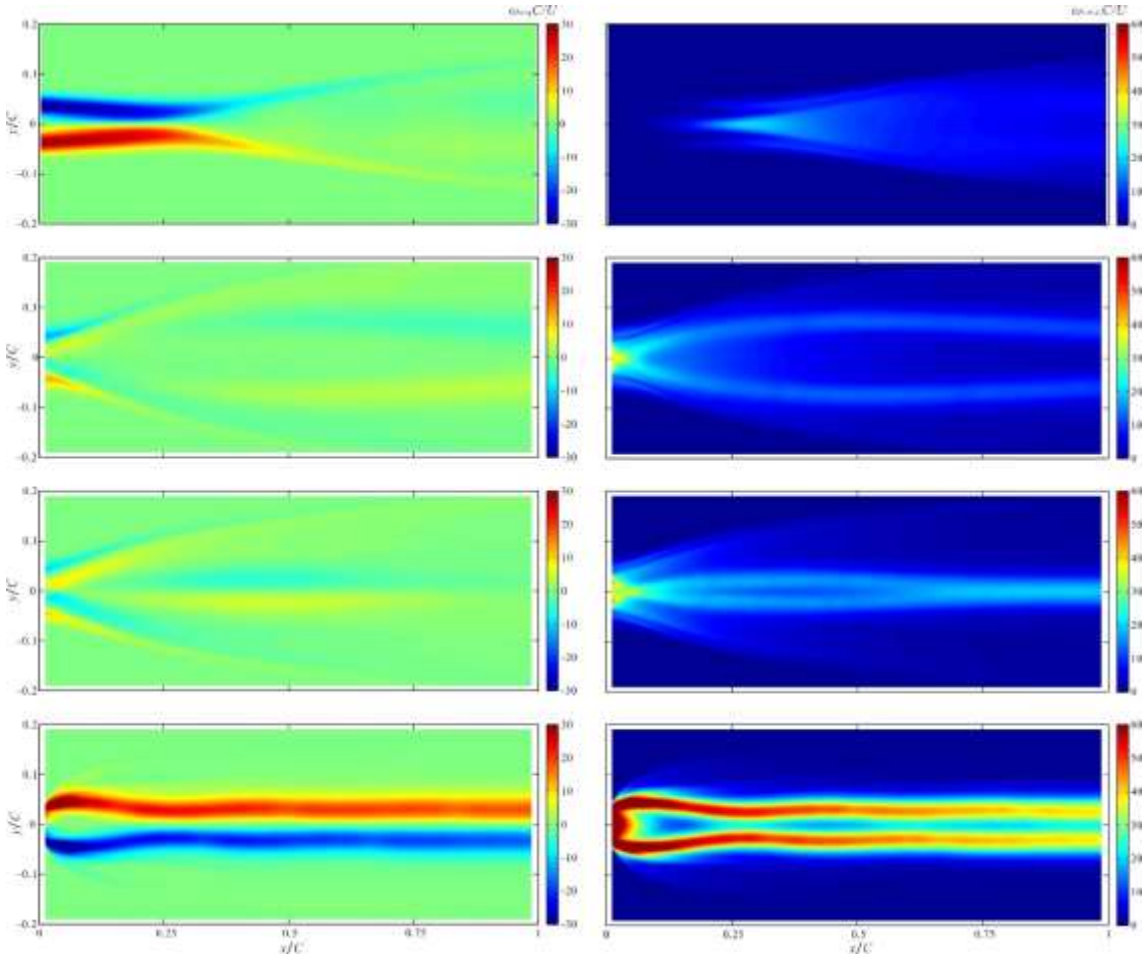

Fig. 4 Mean and r.m.s. vorticity fields, ω_{avg} and $\omega_{r.m.s.}$ in the near wake of static and pitching airfoil

The downstream evolution of vortex spacing as derived from tracking the trajectories of individual vortices is presented to provide a quantitative assessment of the vortical patterns. The computed variation of the transverse coordinates of positive and negative vortices, $y_{c,p}$ and $y_{c,n}$, along with the vortex array transverse spacing is

illustrated in Fig. 5. The variation of of peak vorticity $<\omega_z>_{peak}$ as a function of vortex core downstream location x_c is also demonstrated (see Fig. 6). In the low reduced frequency case (k = 5.2), the positive vortices are initiated at y > 0 whereas the negative vortices are initiated at y < 0. Then, the vortex array start to move towards each other and reaches to an orientation switch at $x/C \approx$ 0.03C. After that, the vortex array moves apart over the first half chord downstream to a maximum spacing of about b = 0.15C before moving back towards each other again and approaching a constant transverse spacing at about x/C = 1 with negative vortex on top. In the high reduced frequency case, the vortex array transverse spacing possesses a oscillatory behavior with a maximum amplitude of only about 0.01C. The oscillation damped out quickly and the vortical pattern attains a transverse spacing with positive vortices on top.

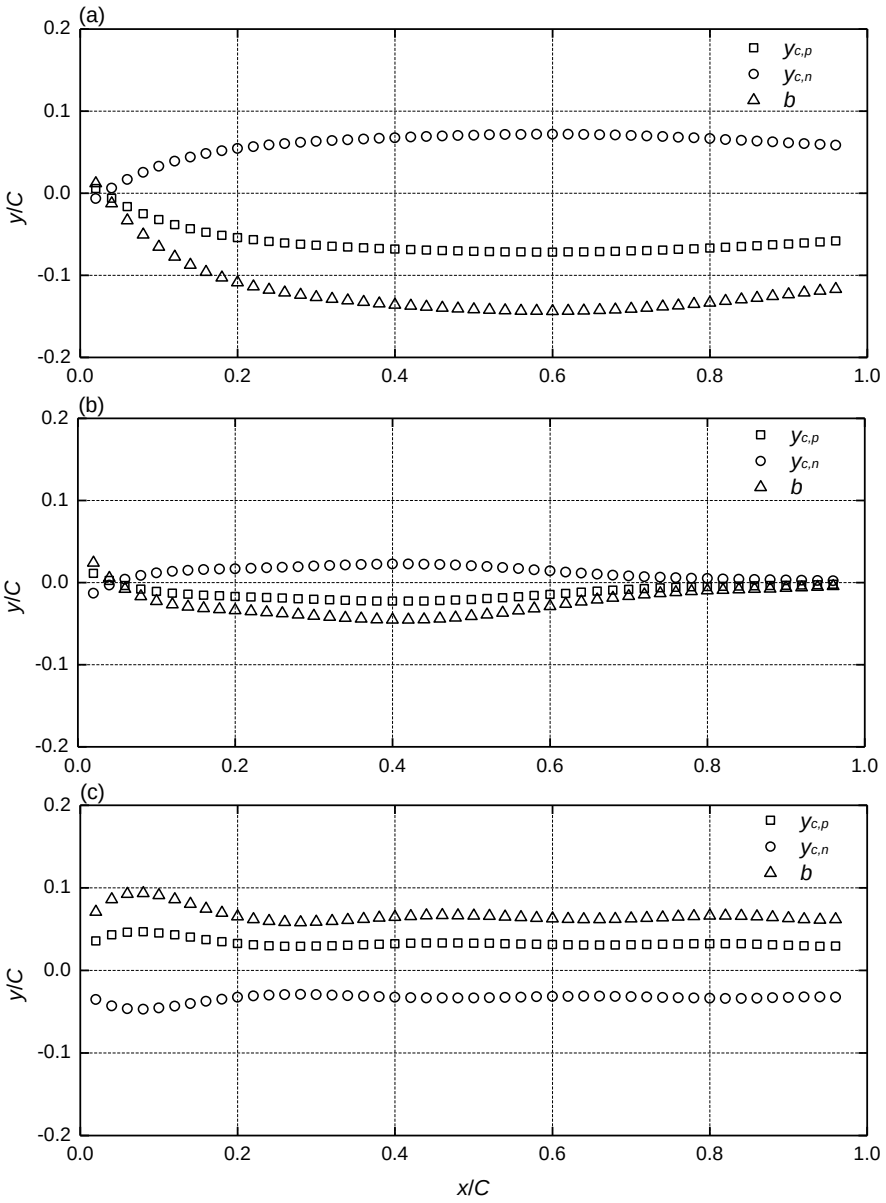

Fig. 5 Downstream evolution of vortex coordinates: (a) k=5.2, (b) k=5.7 and (c) k=11.5

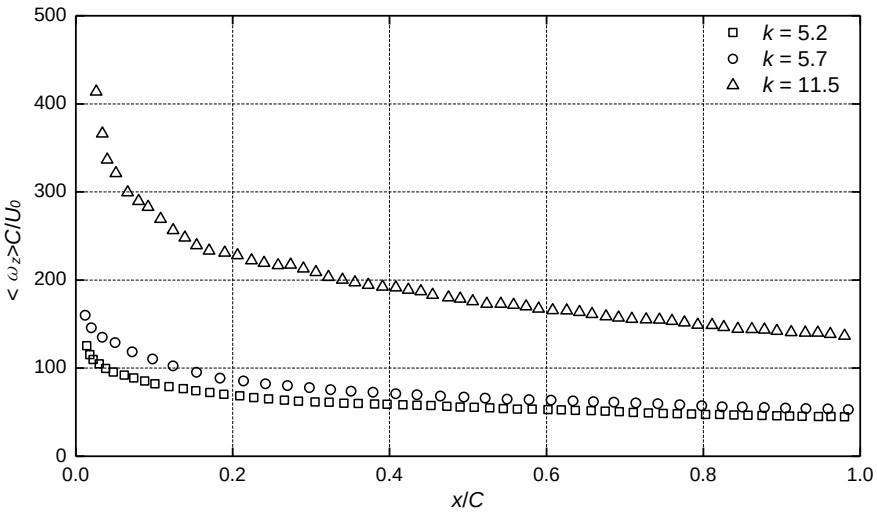

Fig. 6 Peak vorticity $<\omega_z>_{peak}$ as a function of as a function of vortex core downstream location for k = 5.2, 5.7 and 11.5

3.2 Aerodynamics and pressure variations

The streamwise aerodynamic force acting on the pitching airfoil (i.e. drag or thrust) are computed by integrating the surface pressure along the chord surface, and is shown in Fig. 7. The areodynamic hysteresis are also demonstrated as a supplement (Fig. 8). A large increase in thrust peak is identified for reduced frequency k = 11.5 and the thrust peak is found to be reached when the airfoil is at its maximum pitching amplitude. The mean pressure coefficient along the airfoil is also shown (Fig. 9) to explore the connection between drag-to-thrust transition with surface pressure variation. For k = 5.2 or 5.7, the C_P plot resemble that of static foil within almost the entire chord length except for trailing edge where the suction pressure increases. However, for k = 11.5, a significant increase in negative pressure peak is demonstrated which highlights the massive generation of vorticity at this region.

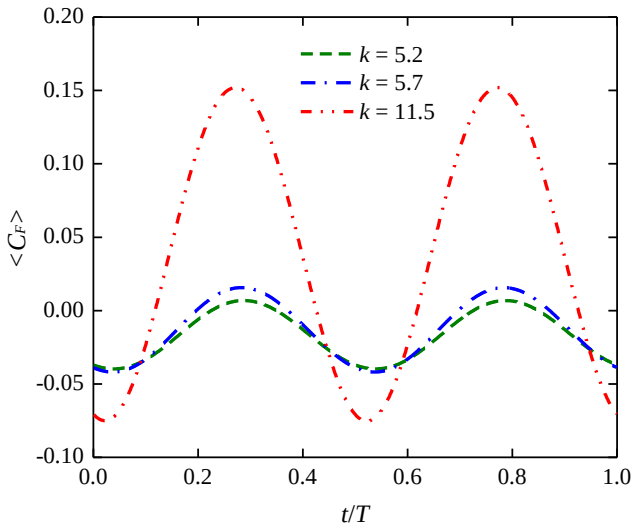

Fig. 7 Time histories of the streamwise force coefficient for k = 5.2, 5.7 and 11.5

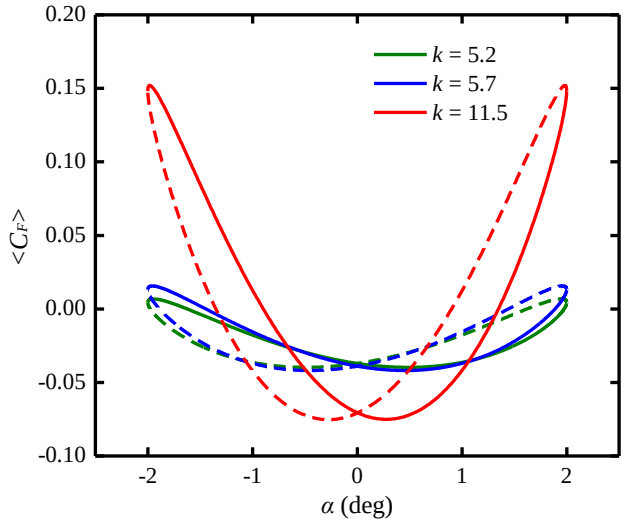

Fig. 8 Aerodynamic hysteresis of the streamwise force coefficient for k = 5.2, 5.7 and 11.5 (solid lines denote upstroke, dashed lines denote downstroke)

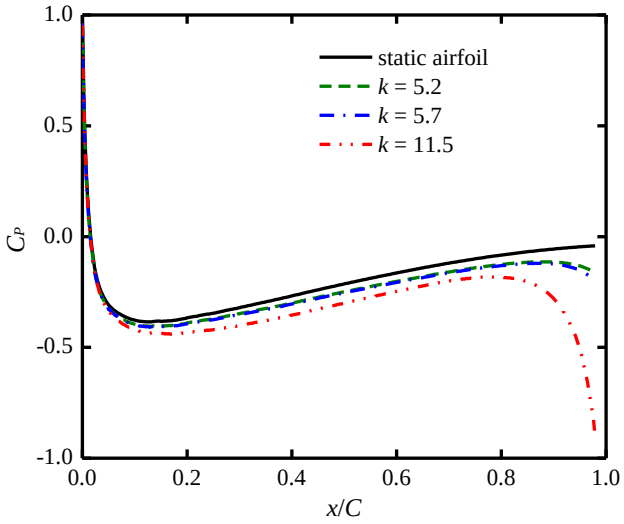

Fig. 9 Mean surface pressure coefficient along the airfoil for k = 5.2, 5.7 and 11.5

4. CONCLUSIONS

The flow field in the near wake of a NACA-0012 airfoil pitching harmonically at small amplitude is numerically simulated in the present study. The characteristics of vortical patterns, i.e. the formulation and downstream evolution of vortex, and its relationship with the reduced frequency are investigated. The pressure variation along the chord surface are also computed to study the connection between wake structure and drag-to-thrust transition. The numerical results highlight the wake structure consists of an array of alternating vortex and its dependence on oscillating frequency. Note that, the transverse location of vortex array changes from an orientation leading to velocity deficit (Von Kármán street with wake profile) to one with velocity excess (reverse Von

Kármán street with jet profile) with increasing reduced frequency. However, the switch from Von Kármán vortex street to reverse Von Kármán vortex street is found to take place ahead of the drag-to-thrust transition.

REFERENCES

Schnipper, T., Andersen, A., Bohr, T. (2009), "Vortex wakes of a flapping foil", *J. Fluid Mech.,* **633**, 411-423.

Jeong, J., Hussain, F. (1995), "On the identification of a vortex", *J. Fluid Mech.,* **285**, 69-94.

Cohn, R. K. & Koochesfahani, M. M. (2000), "The accuracy of remapping irregularly spaced velocity data onto a regular grid and the computation of vorticity", Experiments Fluids **29**, S61.

Koochesfahani, M. M. (1989), "Vortical patterns in the wake of an oscillating airfoil", AIAA J. **27**,1200.

Bohl, D. G. & Koochesfahani, M. M. (2009), "MTV measurements of the vortical field in the wake of an airfoil oscillating at high reduced frequency", J. Fluid Mech. **620**, 63-88.